

Article

Structural Characterization and Immunological Activity of Polysaccharide Degradation Products from *Phlebopus portentosus*

Dan Yu ^{1,2}, Xiaoming Cai ^{1,2}, Shuo Wang ^{1,3}, Yi Li ¹ , Yuguang Du ^{2,4}, Zhuo A. Wang ^{2,4} , Siming Jiao ^{2,4,*} and Zhenquan Yang ^{1,*}

¹ School of Food Science and Engineering, Yangzhou University, Yangzhou 225127, China; yd455YD2014@163.com (D.Y.); xiaomingcai@163.com (X.C.); wangsh@yzu.edu.cn (S.W.); liyi062@yzu.edu.cn (Y.L.)

² State Key Laboratory of Biochemical Engineering, Institute of Process Engineering, Chinese Academy of Sciences, Beijing 100190, China; ygdu@ipe.ac.cn (Y.D.); wangzhuo@ipe.ac.cn (Z.A.W.)

³ Jiangsu Alphas Bio-Technology Co., Ltd., Nantong 226010, China

⁴ Key Laboratory of Biopharmaceutical Preparation and Delivery, Chinese Academy of Sciences, Beijing 100190, China

* Correspondence: smjiao@ipe.ac.cn (S.J.); yangzq@yzu.edu.cn (Z.Y.)

Abstract: *Phlebopus portentosus* is an edible and medicinal mushroom with a delicious taste and high nutritional value. The oligosaccharides derived from *P. portentosus* may be the material basis for its biological activity. The degradation of polysaccharide and the maintenance of its activity after degradation are key steps in related research. This study applied an acid degradation method to prepare *P. portentosus* refined polysaccharide (PPRP) with a smaller molecular weight, and the optimal hydrolysis conditions determined were a temperature of 80 °C, an acid concentration of 2 mol/L, and a hydrolysis time of 2 h. The polysaccharide structure and immune activity were then further investigated. The results showed that the PPRP comprised two fractions with approximate weights of 61,600 Da and 5500 Da. The monosaccharide composition of PPRP was mannose, rhamnose, glucose, and galactose, with a molar ratio of 1.00: 22.24: 2.93: 1.03. The major functional groups included O-H, C-H, C-O, and C-O-C. The glycosidic bond types were mainly α - and β -glycosidic bonds. Cell experiments demonstrated that PPRP could significantly increase the proliferation of macrophages and enhance the cytotoxicity of NK cells. Moreover, PPRP also significantly promoted the proliferation of B lymphocytes and T lymphocytes, especially at a concentration of 200 μ g/mL. This study furnishes scientific evidence underlining the significant potential of PPRP in immune activity, thereby serving as a material basis and scientific bedrock for further investigations into the mechanism of *P. portentosus* oligosaccharide activity.

Keywords: *Phlebopus portentosus*; polysaccharides; acid degradation; structural characterization; immune activity



Citation: Yu, D.; Cai, X.; Wang, S.; Li, Y.; Du, Y.; Wang, Z.A.; Jiao, S.; Yang, Z. Structural Characterization and Immunological Activity of Polysaccharide Degradation Products from *Phlebopus portentosus*. *Separations* **2024**, *11*, 105. <https://doi.org/10.3390/separations11040105>

Academic Editors: Paraskevas D. Tzanavaras and Alberto Barbiroli

Received: 1 February 2024

Revised: 26 March 2024

Accepted: 26 March 2024

Published: 30 March 2024



Copyright: © 2024 by the authors. Licensee MDPI, Basel, Switzerland. This article is an open access article distributed under the terms and conditions of the Creative Commons Attribution (CC BY) license (<https://creativecommons.org/licenses/by/4.0/>).

1. Introduction

For centuries, the consumption of wild mushrooms has been driven by their rich content of polysaccharides, proteins, dietary fiber, essential minerals, and secondary metabolites [1]. These constituents position wild mushrooms as valuable reservoirs for health supplements and pharmaceuticals, showcasing noteworthy immunomodulatory, antimicrobial, anti-inflammatory, antidiabetic, hepatoprotective, anticancer, antioxidant, and antiallergic properties [2–6]. Among these mushrooms, *Phlebopus portentosus* (Berk. & Broome) Boedijn, belonging to the order *Boletales*, stands out as a highly coveted wild edible species thriving in the Xishuangbanna region of Yunnan, China, and Northern Thailand [7,8]. Its fruiting bodies are distinguished by elevated levels of protein, crude

fat, polysaccharides, amino acids, and essential mineral elements. Consequently, *P. portentosus* has been proposed to possess medicinal value, significantly contributing to health benefits [9,10].

Polysaccharides, pivotal contributors to the bioactivities of edible mushrooms, have been extensively studied for structural characterization within the *Boletales* order. For example, Khwanta Kaewnarin et al. extracted bioactive polysaccharides from *P. portentosus* using conventional refluxing extraction (RFE) and ultrasound-assisted extraction (UAE), revealing glucose as the prevalent monosaccharide with both α - and β -glycosidic conformations present [11]. In a recent study, *P. portentosus* polysaccharides (PPPs) were obtained through water–ethanol precipitation and the Sevaga method, unveiling a molecular weight distribution (Mn, Mw, Mp) and a composition of ten monosaccharides [12]. Furthermore, purified *Boletus* polysaccharides confirmed α -glycosidic bonds through nuclear magnetic resonance (NMR) [13]. However, variations in structure and functional properties emerged among *Boletales* polysaccharides obtained through different extraction methods. The reported high molecular weights pose challenges for direct absorption, potentially limiting efficacy. Studies suggest that polysaccharides with lower molecular weights demonstrate superior immune-regulating effects [14]. Therefore, refining methods to degrade and prepare *P. portentosus* polysaccharides with smaller molecular weights is crucial for enhancing their bioactivity.

Concurrently, research on the immune responses induced by *Boletales* polysaccharides has demonstrated significant effects [15]. For instance, Wang et al. discovered significant enhancements in spleen and thymus indices in mice due to *Boletus* polysaccharides. Furthermore, this stimulation extends to spleen cell proliferation and splenic NK cell and CTL activities, setting off an increase in secretions of IL-2 and TNF- α cytokines, all of which imply a potential for immune enhancement [16]. Building on this, Su et al. [17] reported a water-soluble heteropolysaccharide derived from *Boletus reticulatus* Schaeff and noted robust proliferative activity in macrophage RAW 264.7 cells, T cells, and B cells. Additionally, it kindled the secretion of various immunoglobulins, such as IgG, IgE, IgD, and IgM. Moreover, when conducting research on polysaccharides drawn from *Leccinum crocipodium* (Letellier) Watliag, Zheng et al. [18] purified and separated them into three polysaccharides with diverse molecular weights and monosaccharide compositions (LCP-1, LCP-2, and LCP-3). As part of the overall findings, these three purified polysaccharides demonstrated increased immunomodulatory activities, particularly in macrophage RAW 264.7 cells. However, the scope of investigations into the immune responses of *P. portentosus* polysaccharides is limited, and the alterations in immune activity after the degradation of the polysaccharides remain unclear. On the other hand, *P. portentosus* polysaccharides belong to a class of macromolecular substances that are difficult to absorb directly through the gastrointestinal tract. They need to be degraded into oligosaccharides by intestinal microorganisms and enzymes. Therefore, it can be inferred that the material basis of the immunomodulatory activity of *P. portentosus* is probably the oligosaccharide fragment after degradation.

To investigate the structure–activity relationship of *P. portentosus* polysaccharide immunoregulation at the oligosaccharide level, it is imperative to examine the optimal degradation conditions of *P. portentosus* polysaccharides and evaluate their levels of sustained immune activity. Consequently, this research embarked on an initial exploration to degrade *P. portentosus* polysaccharides with the goal of producing polysaccharides of low molecular weight and subsequently estimating their immunomodulatory activity. Acid hydrolysis is set to be utilized to further break down the *P. portentosus* polysaccharides, and the ensuing *P. portentosus* refined polysaccharide (PPRP) will be structurally distinguished and their immunomodulatory activity gauged. The data secured from this project will furnish a solid foundation for future polysaccharide activity studies of *P. portentosus* at the oligosaccharide level.

2. Materials and Methods

2.1. Materials

P. portentosus mushrooms were purchased from Jinghonghongzhen Agricultural Technology Co., Ltd. (Yunnan, China). Series molecular weight dextran standards were purchased from the National Institutes for Food and Drug Control (Beijing, China). Monosaccharide standards (including Man, GalA, Glu, Gal, Xyl, Ara, GluA, Fuc, Rha, GLcN, and GlcNAc) were purchased from Meilun Biotechnology Co., Ltd. (Dalian, China). Papain was purchased from Solarbio (Beijing, China). Trichloroacetic acid and trifluoroacetic acid (TFA) were purchased from Aladdin Biochemical Technology Co., Ltd. (Shanghai, China). 1-phenyl-3-methyl-5-pyrazolinone (PMP) was purchased from Sigma (St. Louis, MO, USA). RPMI-1640 medium was purchased from Wuhan Boster Biological Technology Co., Ltd. (Wuhan, China). Mouse splenic lymphocytes and peritoneal macrophages were purchased from Procell Life Science & Technology Co., Ltd. (Wuhan, China). YAC-1 cells, Concanavalin A (ConA), lipopolysaccharide (LPS), and Cell Counting Kit 8 (CCK-8) were purchased from Beijing Solarbio Science & Technology Co., Ltd. (Beijing, China).

2.2. Extraction of Crude Polysaccharides

P. portentosus crude polysaccharides were extracted by a previously described method [19]. In brief, fresh *P. portentosus* mushrooms were sliced into fragments and dried in a 60 °C oven. The dehydrated fruiting bodies were then pulverized and submitted to aqueous extraction at 90 °C for 4 h under stirring. Subsequently, the aqueous extract was centrifuged, and the supernatant was rotary evaporated and concentrated to one-fourth of the original volume. The polysaccharides were then precipitated overnight at 4 °C by ethanol addition (4:1, *v/v*), and the crude polysaccharides were collected by centrifugation (8000 rpm for 10 min) and lyophilization.

2.3. Purification of Crude Polysaccharides

Crude polysaccharides (20.0 g) were dissolved in 200 mL of ultrapure water, adding 15 mg of papain protease to remove free proteins at 45 °C for 6 h, followed by a 6-min water bath at 100 °C to inactivate the enzyme. After inactivation, 10% of the volume of trichloroacetic acid was added to the solution. The mixture was stirred within an ice bath for 15 min, and then centrifuged at 3000 rpm for 15 min. Subsequently, the resulting supernatant was concentrated by evaporator and precipitated by ethanol addition (9:1, *v/v*), and then allowed to stand overnight at 4 °C. The precipitate was collected and redissolved in hot water before being freeze-dried for further analysis. The phenol–sulfuric acid method determined the total carbohydrate content in the obtained polysaccharides at an absorbance of 496 nm [20].

2.4. Degradation of Crude Polysaccharides

Acid hydrolysis was used to degrade the extracted *P. portentosus* crude polysaccharides. Briefly, 50 mg of crude polysaccharides was dissolved in 10 mL of ultrapure water to prepare a 5 mg/mL sugar solution. Next, various concentrations (0.5–2 mol/L) of TFA were added to the sugar solution for hydrolysis (Table 1). A three-factor, three-level optimization experiment was conducted on the acid hydrolysis conditions for crude polysaccharide extraction from *P. portentosus*. The experimental factors included hydrolysis temperature (60 °C, 70 °C, 80 °C), hydrolysis time (1 h, 2 h, 3 h), and acid concentration (0.5 mol/L, 1.0 mol/L, 2.0 mol/L). The generated monosaccharide quantity and content were utilized as the performance metric to determine the optimal acid hydrolysis condition.

Table 1. Degradation experimental conditions for optimal acid hydrolysis.

Factor	A	B	C	D	E	F	G	H	I
Temperature (°C)	60	60	60	70	70	70	80	80	80
Acid concentration (M)	0.5	1	2	0.5	1	2	2	1	0.5
Time (h)	1	2	3	2	3	1	2	1	3

2.5. Preparation of PPRP

The crude polysaccharide from *P. portentosus* was subjected to degradation using the optimal acid hydrolysis conditions determined in Section 2.4 (80 °C, 2 mol/L TFA, 2 h). After rotary evaporation, the sample was washed twice with methanol to remove residual TFA. Next, the degraded products of crude polysaccharides were redissolved in ultrapure water and filtered through a 0.45 µm membrane, then analyzed using an Alliance E2695 high-performance liquid chromatography (HPLC) system (Waters Corp., Milford, MA, USA) coupled with a charged aerosol detector (CAD, Chromachem, ESA, Inc., Tokyo, Japan). The samples with consistent chromatographic profiles were collected. After concentration and lyophilization, a degraded polysaccharide mixture, named PPRP, was obtained. The chromatographic profiles were as follows: column (X-Amide, 250 mm × 4.6 mm, 5 µm, Acchrom Corp., Beijing, China); eluent (A, ultrapure water; B, acetonitrile); column temperature (35 °C); flow rate (1.0 mL/min); and injection volume (20 µL). The drift tube temperature of ELSD was maintained at 105 °C and nitrogen pressure was controlled at 26 psi.

2.6. Analysis of Structure Characterization of PPRP

2.6.1. Determination of Molecular Weight Distribution

The relative molecular weight of the degraded polysaccharides was measured by high-performance gel filtration chromatography (HPGFC) with a TSK-GMPWXL gel column (7.8 mm × 300 mm, 10 µm, Tosoh Corp., Tokyo, Japan). The chromatographic conditions were as follows: eluent (ultrapure water); column temperature (30 °C); flow rate (0.5 mL/min); drift tube temperature (90 °C); atomizer (N₂) pressure (26 psi); and injection volume (20 µL). Ten standard dextrans (Mw: 180, 2700, 5250, 9750, 13,050, 36,800, 64,650, 135,350, 300,600, and 2,000,000 Da) were used to calibrate the standard curve.

2.6.2. Determination of Monosaccharide Composition

The monosaccharide composition of PPRP was determined from its hydrolytes using an HPLC system equipped with an ultraviolet detector (HPLC-UV, S6000, Acchrom Corp.) [21]. Briefly, 5 mg PPRP was hydrolyzed with 3 mL of 2 mol/L TFA at 120 °C for 2 h in sealed tubes. A rotary vacuum evaporator removed the residual TFA with methanol under reduced pressure. The hydrolytes were redissolved in 1 mL of ultrapure water, mixed with 0.24 mL of 0.5 mol/L PMP and 0.20 mL of 0.3 mol/L sodium hydroxide, and then shaken thoroughly (300 rpm) in a metal bath at 70 °C for 70 min. After cooling, 0.3 mol/L of hydrochloric acid was added for neutralization. The resulting mixture was extracted with 1 mL chloroform, and the upper solution was centrifugally extracted 3 times and then filtered through 0.45 µm membrane for HPLC-UV analysis.

HPLC-UV analysis was performed on Unitary C18 columns (250 mm × 4.6 mm, 5 µm, Acchrom Corp.), in which the eluent consisted of 50 mmol/L potassium dihydrogen phosphate buffer (A) and acetonitrile (B) at a flow rate of 1.0 mL/min. The column temperature was set at 35 °C, the detection wavelength was 250 nm, and the injection volume was 20 µL.

2.6.3. Fourier Transform Infrared (FTIR) Spectroscopy Analysis

The FTIR spectrum of PPRP was measured with an attenuation total reflection FTIR spectrometer (Nicolet™ iS20, Thermo Fisher Scientific). Briefly, 2 mg of PPRP sample was mixed with 100 mg of potassium bromide powder with thorough grinding, and the mixture

was then compressed into tablets. The scanning wavelength was recorded in a range of 4000 cm^{-1} to 450 cm^{-1} .

2.6.4. Nuclear Magnetic Resonance (NMR) Spectroscopy Analysis

Briefly, each dried PPRP sample (30 mg) was dissolved with 1 mL of deuterium oxide (D₂O) at room temperature for 3 h before NMR analysis. High-resolution 1D NMR (¹H NMR and ¹³C NMR) and 2D NMR (HSQC) spectra were recorded separately using an NMR spectrometer (600 MHz Avance III, Bruker, Billerica, MA, USA).

2.7. Immune Activity Analysis

2.7.1. Nonspecific Immune Responses

In nonspecific immune response assessments, DMEM medium (containing 10% FBS and 1% P/S) was used to adjust the concentration of RAW 264.7 macrophage cells to 1×10^6 cells/mL, cultured for 24 h in 96-well plates in an incubator set at 37 °C with 5% CO₂, followed by treatment with 100 μL of PPRP at concentrations ranging from 20 to 250 $\mu\text{g}/\text{mL}$ under sterile conditions for an additional 24 h. Phagocytic activity was determined by measuring optical density (OD) at 540 nm after staining with neutral red and subsequent cell lysis [22]. For mouse spleen lymphocytes, effector cells (1×10^6 cells/mL) and YAC-1 lymphoma cells (2×10^4 cells/mL) were cocultured at a 50:1 ratio. Various concentrations (20–250 $\mu\text{g}/\text{mL}$) of the sample solution were added, and the cells were incubated for 24 h [23]. NK cell cytotoxicity was calculated using the following formula:

$$\text{NK Cell Cytotoxicity (\%)} = [1 - (\text{OD}_S - \text{OD}_E)] / \text{OD}_T \times 100 \quad (1)$$

where OD_S, OD_E, and OD_T represent absorbance values of the sample group, effector cell control group, and target cell control group, respectively. Finally, the results of each group were compared with the results of the control group and graphed.

2.7.2. Specific Immune Responses

The impact on both T and B lymphocytes was assessed following the methodology of previous research, with minor modifications [24]. In brief, RPMI 1640 medium (containing 10% FBS and 1% P/S) was used to adjust the concentration of mouse spleen lymphocytes to 1×10^6 cells/mL, then seeded at 100 μL per well in a 96-well plate and cultured at 37 °C, 5% CO₂ for 24 h. Subsequently, different concentrations (20–250 $\mu\text{g}/\text{mL}$) of PPRP (90 μL) and either ConA (for T lymphocytes) or LPS (for B lymphocytes) (10 μL , 10 $\mu\text{g}/\text{mL}$) were added to the respective wells, and the cells were incubated for an additional 24 h. Post-incubation, 20 μL of CCK-8 was added to each well, and proliferation activity was determined using a microplate reader (SynergyMx, BioTek) at 540 nm, following the instructions of the assay kit.

2.8. Statistical Analysis

All experiments were performed at least three times, and the mean value and standard deviation (SD) were calculated using Microsoft Excel 2016 software. Analysis of variance (ANOVA) was performed using SPSS software (version 22.0, SPSS Inc., Chicago, IL, USA). A *p*-value smaller than 0.05 was considered statistically significant.

3. Results

3.1. Extraction and Purification of Crude Polysaccharides from *P. portentosus*

Using the phenol–sulfuric acid method and Coomassie blue staining to determine total sugar content and protein content, respectively, the crude polysaccharides from *P. portentosus* were found to contain $76.7 \pm 3.1\%$ total carbohydrate content and $22.8 \pm 1.2\%$ protein content. Due to the elevated protein content in the crude polysaccharides, further purification was deemed necessary. Trichloroacetic acid and papain were employed to remove protein impurities from the crude polysaccharides. Following purification, the protein content was

only $1.8 \pm 0.1\%$ and the total carbohydrate content increased to $87.8 \pm 1.1\%$, significantly enhancing the purity of the crude polysaccharides from *P. portentosus* ($p < 0.05$).

3.2. Preparation of PPRP

After protein removal, further preparation of PPRP from the crude polysaccharides of *P. portentosus* involved TFA degradation (Figure 1). As depicted in Figure 1A–C, at a lower temperature of $60\text{ }^{\circ}\text{C}$, increasing acid concentration and hydrolysis time did not yield the ideal monosaccharide peaks in the chromatogram, indicating ineffective degradation of crude polysaccharides. Subsequently, as the temperature increased to $70\text{ }^{\circ}\text{C}$ (Figure 1D–F), it was observed that, despite increasing acid concentration and hydrolysis time, the degradation efficiency remained insufficient. Finally, elevating the temperature to $80\text{ }^{\circ}\text{C}$ (Figure 1G–I) resulted in a notable increase in the number and content of polysaccharide fragments with small molecular weights in the chromatogram, highlighting the significant impact of temperature on the degradation of crude polysaccharides from *P. portentosus*.

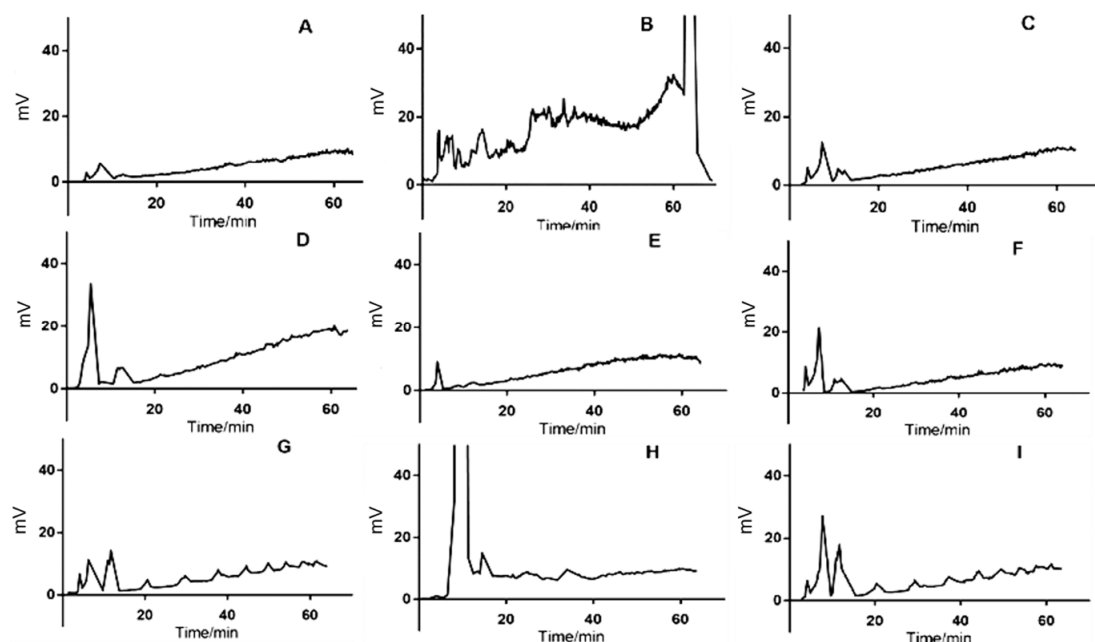


Figure 1. HPLC chromatogram of the acidolysis of *P. portentosus* polysaccharide. The conditions (A–I) in the figure correspond to the temperatures, acid concentrations, and times in Table 1, such as A represents the temperature of $60\text{ }^{\circ}\text{C}$, the acid concentration of 0.5 mol/L , and the time of 1 h.

The chromatography results derived from acid hydrolysis reveal a wide and rich array of polysaccharide fragments with small molecular weights. This serves as a key determinant in choosing the optimal acid hydrolysis condition, thereby ensuring the presence of essential oligosaccharide fragments. Consequently, employing an acid hydrolysis temperature of $80\text{ }^{\circ}\text{C}$, an acid concentration of 2 mol/L , and a hydrolysis duration of 2 h (Figure 1G) results in a stable baseline and an optimal peak shape for the polysaccharide fragment with a small molecular weight. In comparison to Figure 1I, this method is more time-efficient, with the single-peak effect notably improving around the 60-min mark. Thus, given these advantages, the conditions represented in Figure 1G were identified as the optimal preparation parameters for PPRP. These conditions were then applied to the ongoing preparation of PPRP.

3.3. Structural Characterization of PPRP

3.3.1. Molecular Weight

The molecular weight distribution of PPRP was assessed using HPGFC, employing the linear regression equation $\log Mw = -0.5514t_R + 15.026$ ($R^2 = 0.997$) derived from the dextroside control. Molecular weight analysis revealed that PPRP comprised two fractions with approximate weights of 62,000 Da and 5500 Da (Figure 2A). In a comparable study, Zheng et al. employed a similar preparation method to produce a *Boletus* polysaccharide, yielding a measured molecular weight of 1.79×10^6 Da, surpassing that of PPRP [25]. This discrepancy suggests the successful preparation of a refined polysaccharide with a lower molecular weight in the present study.

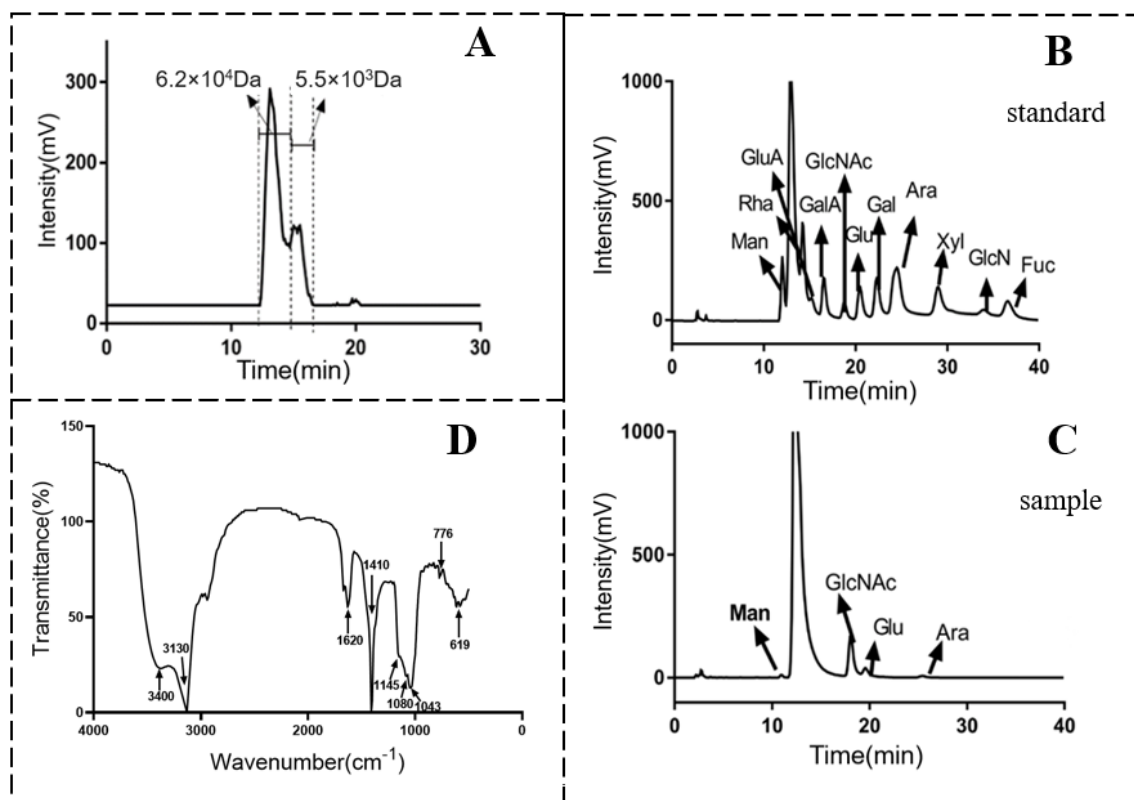


Figure 2. Structural characterization of PPRP. Molecular weight distribution chromatogram of PPRP measured by HPGFC with a TSK–GMPWXL gel column (A). HPLC chromatogram of standard monosaccharide mixtures (B). Monosaccharide composition of PPRP determined by HPLC chromatogram (C). Chemical bonding results of PPRP measured by FT–IR spectra (D).

3.3.2. Monosaccharide Composition

Utilizing precolumn derivatization with PMP followed by HPLC, the chromatograms of 11 standard monosaccharide mixtures (Figure 2B) and the monosaccharide composition of PPRP (Figure 2C) were determined. Comparative analysis revealed that PPRP primarily consists of Man, GlcNAc, Glu, and Ara. When normalized to a unit quantity of Man, the molar ratio of Man:GlcNAc:Glu:Ara was calculated as 1.00:22.24:2.93:1.03. GlcNAc exhibited the highest content, significantly surpassing other monosaccharides and establishing it as the predominant sugar component in PPRP.

3.3.3. FT–IR Spectrum

Chemical bonding analysis of PPRP was conducted using FT–R spectroscopy (Figure 2D). As shown, the FT–IR spectrum of PPRP exhibits major characteristic absorption peaks associated with polysaccharides. The peak around 3400 cm^{-1} corresponds to the

stretching vibration of —O—H bonds in polysaccharides. At approximately 3130 cm^{-1} , the absorption peak is attributed to the stretching vibration of C—H bonds in carbohydrates. The peak around 1620 cm^{-1} represents the stretching vibration of the carbonyl group after carbohydrate molecules undergo ring-opening. The strong characteristic absorption peak at about 1410 cm^{-1} arises from the deformation vibration of C—H bonds. Between 1145 and 1043 cm^{-1} , three absorption peaks indicate stretching vibrations of C—O—C and C—O—H in carbohydrate rings, suggesting the presence of pyranose glycosides. The absorption peak at around 619 cm^{-1} is characteristic of an α -pyranoside bond [26], while the peak at approximately 776 cm^{-1} is characteristic of a β -pyranoside bond [27,28].

3.3.4. NMR Spectrum

The 1D/2D NMR spectra of PPRP are shown in Figure 3. The ^1H -NMR spectrum primarily addresses the configuration of glycosidic bonds, allowing for the determination of whether a homogeneous polysaccharide contains a six-membered pyranose or a five-membered furanose ring. The ^1H NMR spectrum has four anomeric proton signals within the range of δ 4.7–5.5 ppm, confirming that PPRP is largely composed of four types of sugar. The chemical shift at δ 4.79 ppm is the peak of D_2O . The combined use of ^{13}C NMR and HSQC provided better attribution analyses of hydrogen signals on heteroatomic carbons in the proton spectrum and other positions. In the carbon spectrum of PPRP, peaks in the range of 90–100 ppm correspond to heteroatomic carbons. Combined with HSQC, it was determined that the hydrogen peaks on heteroatomic carbons fall between 4.50 and 5.36 ppm in the proton spectrum, indicating the presence of both α - and β -glycosidic bonds in PPRP. The signal at δH 1.16–1.21 ppm suggests the presence of a C—CH_3 structure in PPRP.

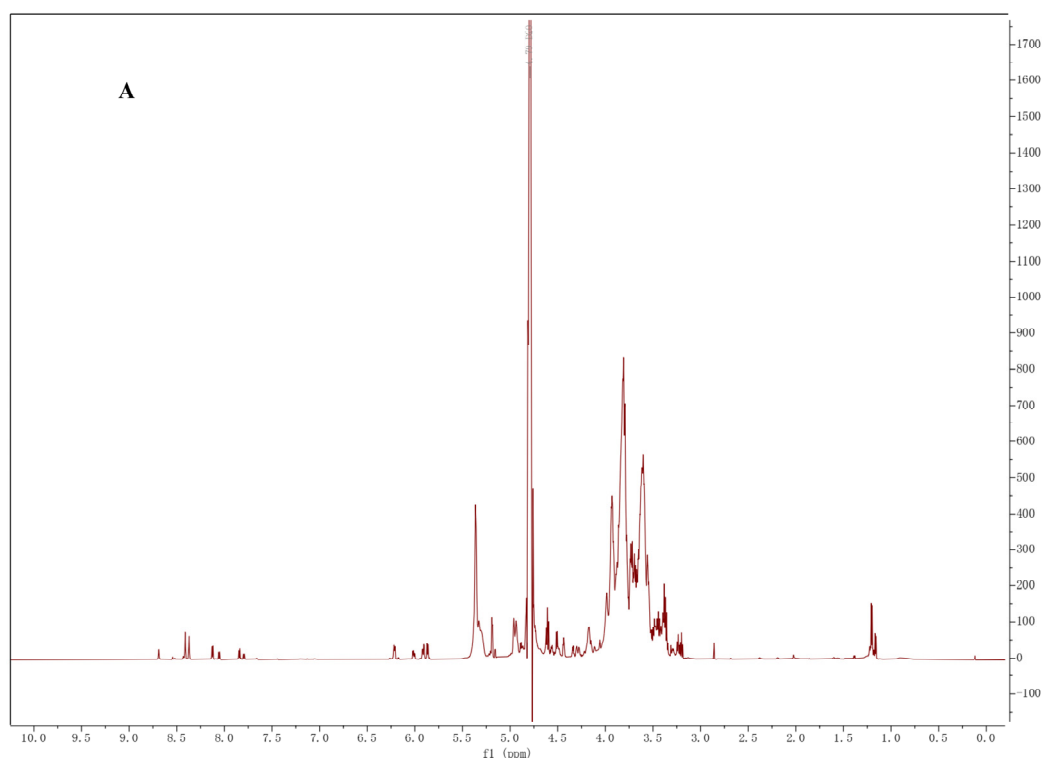


Figure 3. Cont.

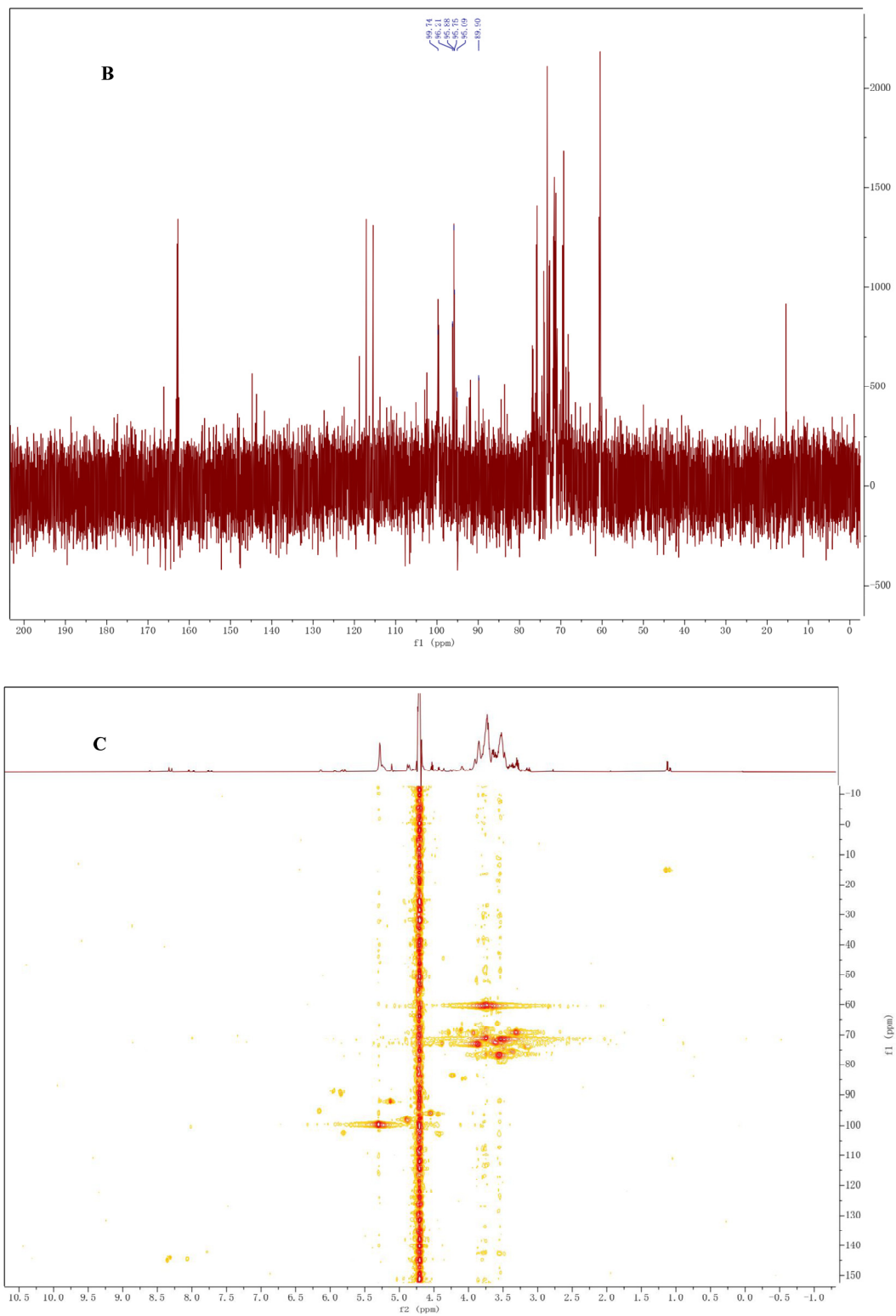


Figure 3. Results of the NMR spectrum analysis. ^1H NMR spectra of PPRP (A). ^{13}C NMR spectra of PPRP (B). HSQC spectra of PPRP (C).

3.4. Immune Response

3.4.1. Effects of PPRP on Nonspecific Immune Response

In this experiment, the proliferation rate of RAW 264.7 macrophages and the cytotoxic effect on NK cells were used as indicators to investigate the nonspecific immune responses of PPRP at concentrations of 20 µg/mL, 50 µg/mL, 100 µg/mL, 150 µg/mL, 200 µg/mL, and 250 µg/mL, as shown in Figure 4.

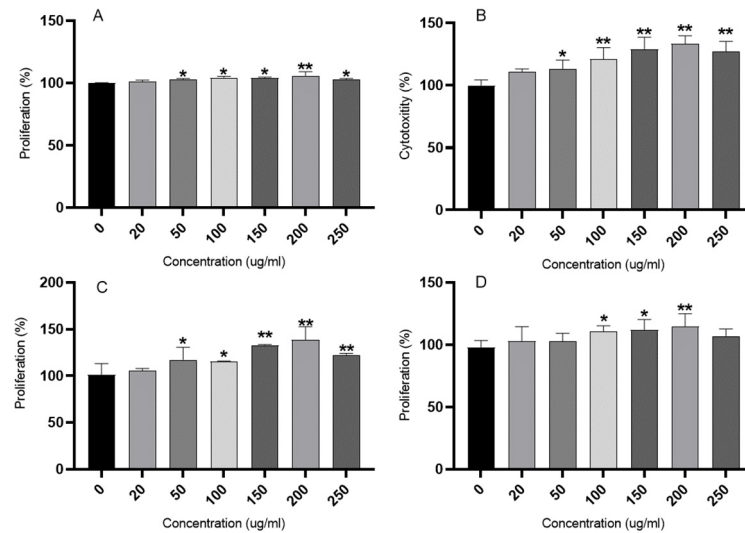


Figure 4. Immunoactivity evaluation results for different concentrations of PPRP. * denotes $p < 0.05$; ** denotes $p < 0.01$. The proliferation rate of RAW 264.7 macrophages (A). The cytotoxic effect of NK cells (B). The proliferation rate of B lymphocytes (C). The proliferation rate of T lymphocytes (D).

Using the proliferation rate of RAW 264.7 macrophages without added PPRP (0 µg/mL) as the control group, the impacts of different concentrations of PPRP on macrophage proliferation activity were analyzed. As depicted in Figure 4A, at a PPRP concentration of 20 µg/mL, there was no significant change in the proliferation rate of macrophages ($p > 0.05$). However, as the PPRP concentration increased to 50 µg/mL, the proliferation rate of macrophages significantly increased (102.93%, $p < 0.05$), and the proliferative effect increased with the improving PPRP concentration, reaching the highest proliferation rate at a PPRP concentration of 200 µg/mL (105.98%).

Similarly, using the cytotoxic effect of NK cells without added PPRP (0 µg/mL) as the control group, the varying impacts of different concentrations of PPRP on NK cell cytotoxicity were compared. As shown in Figure 4B, at an added PPRP concentration of 20 µg/mL, there was no significant change in the cytotoxic effect of NK cells ($p > 0.05$). Subsequently, at a PPRP concentration of 50 µg/mL, a significant cytotoxic effect on NK cells began to appear (113.20%, $p < 0.05$), and the cytotoxic effect increased with concentration ($p < 0.01$), reaching its maximum at a PPRP concentration of 200 µg/mL (133.40%).

However, with further increase in PPRP concentration, it was observed that at 250 µg/mL (102.99% for macrophages; 127.20% for NK cells), both the proliferative effect of macrophages and the cytotoxic effect of NK cells started to decline. This phenomenon may be attributed to the higher osmotic pressure of the high-concentration PPRP solution, leading to the inhibition of macrophage and NK cell activity. It is also possible that the induction of macrophages and NK cells by high concentrations of PPRP resulted in overactivation, leading to cellular dysfunction [29]. Above all, PPRP significantly enhances the proliferation rate of macrophages and the cytotoxic effect of NK cells, indicating its positive impact on enhancing the body’s nonspecific immune response capacity, consistent with previous findings reported by Su et al. [17].

3.4.2. Effects of Refined Polysaccharide on Specific Immune Response

Further, using the proliferation rates of B lymphocytes and T lymphocytes as indicators, the specific immune responses of different concentrations of PPRP (20 µg/mL, 50 µg/mL, 100 µg/mL, 150 µg/mL, 200 µg/mL, and 250 µg/mL) were evaluated, as shown in Figure 4C,D.

Taking the proliferation rate of B lymphocytes without adding PPRP (0 µg/mL) as the control, the impact of different concentrations of PPRP on the proliferation of B lymphocytes was first analyzed. As shown in Figure 4C, the lower concentrations of PPRP (20 µg/mL) had no significant effect on the proliferation of B lymphocytes ($p > 0.05$). However, as the PPRP concentration increased between 50 µg/mL and 100 µg/mL, it began to promote the proliferation of B lymphocytes (117.19% for 50 µg/mL; 115.77% for 100 µg/mL; $p < 0.05$). The proliferation effect became more significant at a PPRP concentration of 150 µg/mL (133.05%, $p < 0.01$), reaching its maximum at 200 µg/mL (138.87%).

Similarly, using the proliferation rate of T lymphocytes without adding PPRP (0 µg/mL) as the control, the impacts of different concentrations of PPRP on the proliferation of T lymphocytes were analyzed (Figure 4D). The proliferation rate of T lymphocytes showed no significant change at PPRP concentrations below 100 µg/mL (20 µg/mL and 50 µg/mL, $p > 0.05$). With a further increase in PPRP concentration to 100 µg/mL, the proliferation rate of T lymphocytes began to significantly increase (110.97%, $p < 0.05$), reaching its maximum at a PPRP concentration of 200 µg/mL (114.91%). Similar to the nonspecific immune response, as the PPRP concentration exceeded 200 µg/mL, a decline in the proliferation effects of B lymphocytes (122.55% for 250 µg/mL) and T lymphocytes (106.97% for 250 µg/mL) was observed, consistent with the results previously reported by Zhu et al. [30]. This decline may be attributed to the higher osmotic pressure of the high-concentration PPRP solution inhibiting cellular activity. In conclusion, the specific immune response results indicate that PPRP significantly promotes the proliferation of B lymphocytes and T lymphocytes within a certain concentration range (100–200 µg/mL), exerting a positive promoting effect on the enhancement of the body's specific immune response capacity.

4. Conclusions

This study embarked upon a meticulous investigation into the optimal hydrolysis conditions for *P. portentosus* polysaccharides, ultimately resulting in the fabrication of *P. portentosus* refined polysaccharide (PPRP) of low molecular weight by utilizing the optimally derived conditions. The structure of PPRP was intensely characterized by employing robust analytical techniques, such as HPGFC, HPLC, FTIR, and NMR. In vitro cellular trials underscored the immunomodulatory efficacy of PPRP. The results showcased its influential role in both nonspecific and specific immunity, thus highlighting its potential contribution to overall health maintenance. Despite these strides, it must be acknowledged that the study did not fully explore all possible benefits of PPRP. More precisely, in vivo animal experiments remain an uncharted territory. Consequently, future research endeavors should lean toward further validation of activity, specifically focusing on systematically dissecting the structure–activity relationship governing the biological effects of PPRP at the oligosaccharide level. Such a targeted approach will holistically encapsulate the potential of PPRP, facilitating further developments within nutritional science.

Author Contributions: All authors participated in conducting analyses, editing, and approving the final submitted version. Conceptualization, supervision, and funding acquisition, Z.Y. and Y.L.; Project administration, S.J.; Methodology, S.W., Y.L., Y.D. and S.J.; Validation, Y.D. and Z.A.W.; Formal analysis, X.C.; Investigation, D.Y. and Y.L.; Resources, Y.L. and S.J.; Data curation, S.W. and Z.A.W.; Writing of the original draft, D.Y. and X.C.; Writing review & editing, S.W., Y.D., Z.A.W. and S.J. All authors have read and agreed to the published version of the manuscript.

Funding: This study was supported by the National Key R&D Program of China [No. 2023YFC2308000] and the Investigation of Wild Germplasm Resources of Agricultural Microorganisms (Edible Fungi) in Jiangsu Province (JSZC-202310261642).

Institutional Review Board Statement: Committee on the Ethics of Animal Experiments of Yangzhou University [Approval ID: SYXK (Su) 2022-0044]. The date of the approval is from 15 July 2022 to 14 July 2027.

Data Availability Statement: Data are contained within the article.

Conflicts of Interest: Author Shuo Wang was employed by the company Jiangsu Alphay Bio-Technology Co., Ltd. The remaining authors declare that the research was conducted in the absence of any commercial or financial relationships that could be construed as a potential conflict of interest.

References

1. Rizzo, G.; Goggi, S.; Giampieri, F.; Baroni, L. A review of mushrooms in human nutrition and health. *Trends Food Sci. Technol.* **2021**, *117*, 60–73. [\[CrossRef\]](#)
2. Wang, X.-M.; Zhang, J.; Wu, L.-H.; Zhao, Y.-L.; Li, T.; Li, J.-Q.; Wang, Y.-Z.; Liu, H.-G. A mini-review of chemical composition and nutritional value of edible wild-grown mushroom from China. *Food Chem.* **2014**, *151*, 279–285. [\[CrossRef\]](#) [\[PubMed\]](#)
3. Ren, L.; Perera, C.; Hemar, Y. Antitumor activity of mushroom polysaccharides: A review. *Food Funct.* **2012**, *3*, 1118–1130. [\[CrossRef\]](#) [\[PubMed\]](#)
4. Jiang, X.; Meng, W.; Li, L.; Meng, Z.; Wang, D. Adjuvant therapy with mushroom polysaccharides for diabetic complications. *Front. Pharmacol.* **2020**, *11*, 168. [\[CrossRef\]](#) [\[PubMed\]](#)
5. Zaki, A.H.; Zahid, M.T.; Haiying, B. Bioactive Compounds of the Culinary-Medicinal Mushroom *Leucocalocybe mongolica* (Agaricomycetes): Pharmacological and Therapeutic Applications—A Review. *Int. J. Med. Mushrooms* **2022**, *24*, 19–33. [\[CrossRef\]](#) [\[PubMed\]](#)
6. Arunachalam, K.; Sreeja, P.S.; Yang, X. The antioxidant properties of mushroom polysaccharides can potentially mitigate oxidative stress, beta-cell dysfunction and insulin resistance. *Front. Pharmacol.* **2022**, *13*, 874474. [\[CrossRef\]](#) [\[PubMed\]](#)
7. Zhang, C.; He, M.; Liu, J.; Xu, X.; Cao, Y.; Gao, F.; Fang, Y.; Wang, W.; Wang, Y. Brief introduction to a unique edible *Bolete-Phlebopus portentosus* in Southern China. *J. Agric. Sci. Technol.* **2017**, *7*, 386–394.
8. Wang, L.; Li, J.; Li, T.; Liu, H.; Wang, Y. Method Superior to Traditional Spectral Identification: FT-NIR Two-Dimensional Correlation Spectroscopy Combined with Deep Learning to Identify the Shelf Life of Fresh *Phlebopus portentosus*. *ACS Omega* **2021**, *6*, 19665–19674. [\[CrossRef\]](#) [\[PubMed\]](#)
9. Sun, Z.; Hu, M.; Sun, Z.; Zhu, N.; Yang, J.; Ma, G.; Xu, X. Pyrrole alkaloids from the edible mushroom *Phlebopus portentosus* with their bioactive activities. *Molecules* **2018**, *23*, 1198. [\[CrossRef\]](#) [\[PubMed\]](#)
10. Kumla, J.; Suwannarach, N.; Tanreuan, K.; Lumyong, S. Comparative evaluation of chemical composition, phenolic compounds, and antioxidant and antimicrobial activities of tropical Black Bolete mushroom using different preservation methods. *Foods* **2021**, *10*, 781. [\[CrossRef\]](#) [\[PubMed\]](#)
11. Kaewnarin, K.; Suwannarach, N.; Kumla, J.; Choopicharn, S.; Tanreuan, K.; Lumyong, S. Characterization of polysaccharides from wild edible mushrooms from Thailand and their antioxidant, antidiabetic, and antihypertensive activities. *Int. J. Med. Mushrooms* **2020**, *22*, 221–233. [\[CrossRef\]](#) [\[PubMed\]](#)
12. Li, H.-F.; Pan, Z.-C.; Chen, J.-M.; Zeng, L.-X.; Xie, H.-J.; Liang, Z.-Q.; Wang, Y.; Zeng, N.-K. Green synthesis of silver nanoparticles using *Phlebopus portentosus* polysaccharide and their antioxidant, antidiabetic, anticancer, and antimicrobial activities. *Int. J. Biol. Macromol.* **2024**, *254*, 127579. [\[CrossRef\]](#) [\[PubMed\]](#)
13. Zhu, Y.; Li, L.; Jin, X.; Li, Z.; Wang, C.; Teng, L.; Li, Y.; Zhang, Y.; Wang, D. Structure characterisation of polysaccharides purified from *Boletus aereus* Bull. and its improvement on AD-like behaviours via reliving neuroinflammation in APP/PS1 mice. *Int. J. Biol. Macromol.* **2024**, *258*, 128819. [\[CrossRef\]](#) [\[PubMed\]](#)
14. Sun, L.; Wang, L.; Zhou, Y. Immunomodulation and antitumor activities of different-molecular-weight polysaccharides from *Porphyridium cruentum*. *Carbohydr. Polym.* **2012**, *87*, 1206–1210. [\[CrossRef\]](#)
15. Li, X.; Yu, L.; Xie, Y.; Li, C.; Fang, Z.; Hu, B.; Wang, C.; Chen, S.; Wu, W.; Li, X.; et al. Effect of different cooking methods on the nutrient, and subsequent bioaccessibility and biological activities in *Boletus auripes*. *Food Chem.* **2023**, *405*, 134358. [\[CrossRef\]](#) [\[PubMed\]](#)
16. Wang, D.; Sun, S.-Q.; Wu, W.-Z.; Yang, S.-L.; Tan, J.-M. Characterization of a water-soluble polysaccharide from *Boletus edulis* and its antitumor and immunomodulatory activities on renal cancer in mice. *Carbohydr. Polym.* **2014**, *105*, 127–134. [\[CrossRef\]](#) [\[PubMed\]](#)
17. Su, S.; Ding, X.; Hou, Y.; Liu, B.; Du, Z.; Liu, J. Structure elucidation, immunomodulatory activity, antitumor activity and its molecular mechanism of a novel polysaccharide from *Boletus reticulatus* Schaeff. *Food Sci. Hum. Wellness* **2023**, *12*, 647–661. [\[CrossRef\]](#)

18. Zheng, T.; Gu, D.; Wang, X.; Shen, X.; Yan, L.; Zhang, W.; Pu, Y.; Ge, C.; Fan, J. Purification, characterization and immunomodulatory activity of polysaccharides from *Leccinum crocipodium* (Letellier.) Watliag. *Int. J. Biol. Macromol.* **2020**, *148*, 647–656. [[CrossRef](#)] [[PubMed](#)]
19. Kakar, M.U.; Naveed, M.; Saeed, M.; Zhao, S.; Rasheed, M.; Firdoos, S.; Manzoor, R.; Deng, Y.; Dai, R. A review on structure, extraction, and biological activities of polysaccharides isolated from *Cyclocarya paliurus* (Batalin) Iljinskaja. *Int. J. Biol. Macromol.* **2020**, *156*, 420–429. [[CrossRef](#)] [[PubMed](#)]
20. Wang, W.; Tan, J.; Nima, L.; Sang, Y.; Cai, X.; Xue, H. Polysaccharides from fungi: A review on their extraction, purification, structural features, and biological activities. *Food Chem. X* **2022**, *15*, 100414. [[CrossRef](#)] [[PubMed](#)]
21. Liu, D.; Tang, W.; Yin, J.-Y.; Nie, S.-P.; Xie, M.-Y. Monosaccharide composition analysis of polysaccharides from natural sources: Hydrolysis condition and detection method development. *Food Hydrocoll.* **2021**, *116*, 106641. [[CrossRef](#)]
22. Wang, J.; Nie, S.; Cui, S.; Wang, Z.; Phillips, A.O.; Phillips, G.O.; Li, Y.; Xie, M. Structural characterization and immunostimulatory activity of a glucan from natural *Cordyceps sinensis*. *Food Hydrocoll.* **2017**, *67*, 139–147. [[CrossRef](#)]
23. Gu, B.; You, J.; Li, Y.; Duan, C.; Fang, M. Enteric-coated garlic supplement markedly enhanced normal mice immunocompetence. *Eur. Food Res. Technol.* **2010**, *230*, 627–634. [[CrossRef](#)]
24. Cai, G.; Wu, C.; Zhu, T.; Peng, S.; Xu, S.; Hu, Y.; Liu, Z.; Yang, Y.; Wang, D. Structure of a Pueraria root polysaccharide and its immunoregulatory activity on T and B lymphocytes, macrophages, and immunosuppressive mice. *Int. J. Biol. Macromol.* **2023**, *230*, 123386. [[CrossRef](#)] [[PubMed](#)]
25. Zheng, J.; Zhang, T.; Fan, J.; Zhuang, Y.; Sun, L. Protective effects of a polysaccharide from *Boletus aereus* on S180 tumor-bearing mice and its structural characteristics. *Ind. Crops Prod.* **2021**, *188*, 1–10. [[CrossRef](#)] [[PubMed](#)]
26. Luo, Q.; Tang, Z.; Zhang, X.; Zhong, Y.H.; Yao, S.Z.; Wang, L.S.; Lin, C.W.; Luo, X. Chemical properties and antioxidant activity of a water-soluble polysaccharide from *Dendrobium officinale*. *Int. J. Biol. Macromol.* **2016**, *89*, 219–227. [[CrossRef](#)] [[PubMed](#)]
27. Xu, Y.; Niu, X.; Liu, N.; Gao, Y.; Wang, L.; Xu, G.; Li, X.; Yang, Y. Characterization, antioxidant and hypoglycemic activities of degraded polysaccharides from blackcurrant (*Ribes nigrum* L.) fruits. *Food Chem.* **2018**, *243*, 26–35. [[CrossRef](#)] [[PubMed](#)]
28. Tang, H.; Wei, W.; Wang, W.; Zha, Z.; Li, T.; Zhang, Z.; Luo, C.; Yin, H.; Huang, F.; Wang, Y. Effects of cultured *Cordyceps mycelia* polysaccharide A on tumor neurosis factor- α induced hepatocyte injury with mitochondrial abnormality. *Carbohydr. Polym.* **2017**, *163*, 43–53. [[CrossRef](#)] [[PubMed](#)]
29. He, Y.; Huang, S.; Xu, G.; Jiang, P.; Huang, L.; Sun, C.; Jin, J.; Chen, C. Structural characteristics and immunomodulation activity of a polysaccharide from purslane (*Portulaca oleracea*). *J. Funct. Foods* **2023**, *109*, 105781. [[CrossRef](#)]
30. Zhu, H.; Ding, X.; Hou, Y.; Li, Y.; Wang, M. Structure elucidation and bioactivities of a new polysaccharide from Xiaojin *Boletus speciosus* Frost. *Int. J. Biol. Macromol.* **2019**, *126*, 697–716. [[CrossRef](#)] [[PubMed](#)]

Disclaimer/Publisher’s Note: The statements, opinions and data contained in all publications are solely those of the individual author(s) and contributor(s) and not of MDPI and/or the editor(s). MDPI and/or the editor(s) disclaim responsibility for any injury to people or property resulting from any ideas, methods, instructions or products referred to in the content.